

SUPPLEMENTARY MATERIAL

Carbon source-dependent reprogramming of anaerobic metabolism in *Staphylococcus aureus*

Running title: Carbon source control of fermentation in *S. aureus*

Anne Troitzsch^a, Vu Van Loi^b, Karen Methling^c, Daniela Zühlke^a, Michael Lalk^c, Katharina Riedel^a, Jörg Bernhardt^a, Eslam M. Elsayed^d, Gert Bange^d, Haike Antelmann^b and Jan Pané-Farré^{a,d#}

- a) University of Greifswald, Department of Microbial Physiology and Molecular Biology, Felix-Hausdorff-Str. 8, 17487 Greifswald, Germany.
- b) Freie Universität Berlin, Institute of Biology-Microbiology, 14195 Berlin, Germany.
- c) University of Greifswald, Institute for Biochemistry, Felix-Hausdorff-Str. 4, 17487 Greifswald, Germany.
- d) Philipps-University Marburg, Center for Synthetic Microbiology (SYNMIKRO) and Department of Chemistry, 35043 Marburg, Germany.

#) Corresponding author:

Jan Pané-Farré

University of Greifswald

Department of Microbial Physiology and Molecular Biology

Felix-Hausdorff-Str. 8

17487 Greifswald, Germany

jan.panefarre@chemie.uni-marburg.de

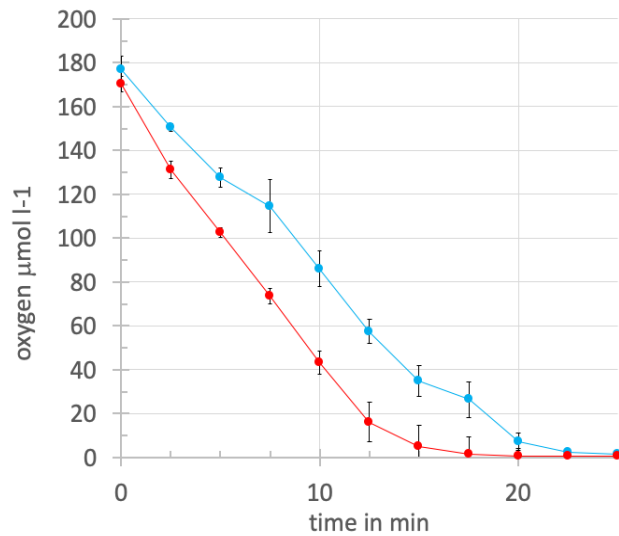


Figure S1. **Oxygen consumption of cells grown in chemically defined medium with glucose (blue circles) or pyruvate (red circles) as major carbon source.** Cells from an exponential overnight culture were transferred to fresh prewarmed medium to yield a start $OD_{500\text{ nm}}$ of 0.075 and grown to an $OD_{500\text{ nm}}$ of 0.5 at 37 °C with agitation (120 rpm). At an $OD_{500\text{ nm}}$ of 0.5 seven ml of the culture were transferred to seven ml airtight screw tubes equipped with oxygen sensor spots (PreSens, Germany). Cells were statically incubated at 37 °C. O_2 -saturation of the cell culture was monitored in 2.5 min intervals for a total of 25 min, within which the oxygen was completely used by the cells. Using information provided by the manufacture, O_2 saturation was converted into $\mu\text{mol } O_2 \text{ l}^{-1}$ values. Error bars show standard deviation of four independent biological replicates.

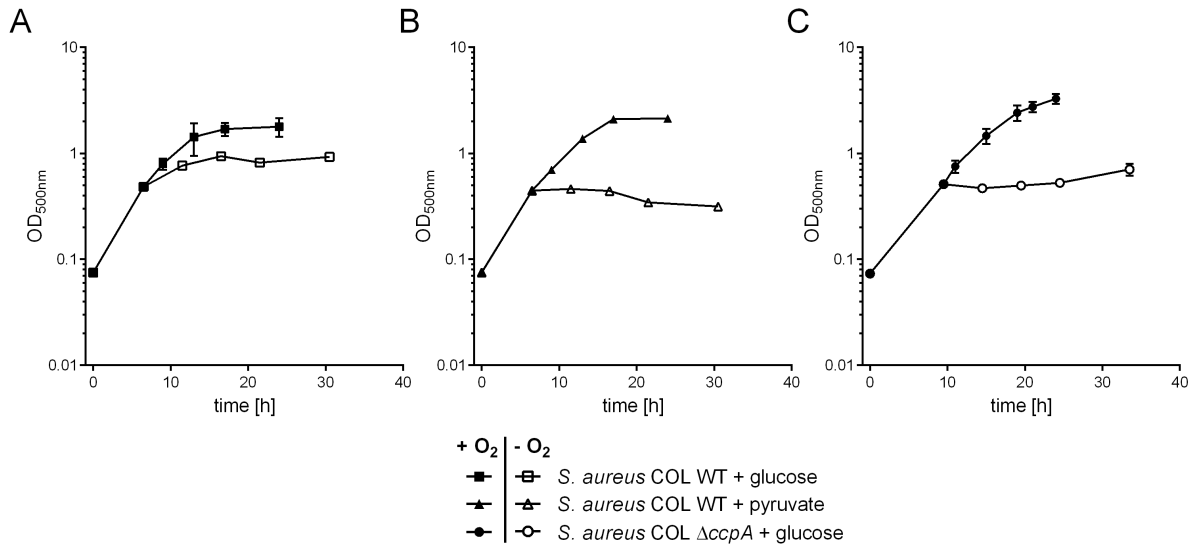


Figure S2. **Carbon source-, oxygen- and *ccpA*-dependent growth of *S. aureus*.** Growth of wild type *S. aureus* COL (squares, triangles) and the isogenic *ccpA* mutant (circles) in chemically defined medium cultured under aerobic conditions (closed symbols) or after a shift to hypoxic conditions at an OD₅₀₀ = 0.5 (open symbols). Cells were grown on glucose (squares) or pyruvate (triangles) as major carbon source. OD values are means with standard deviations of three biological replicates.

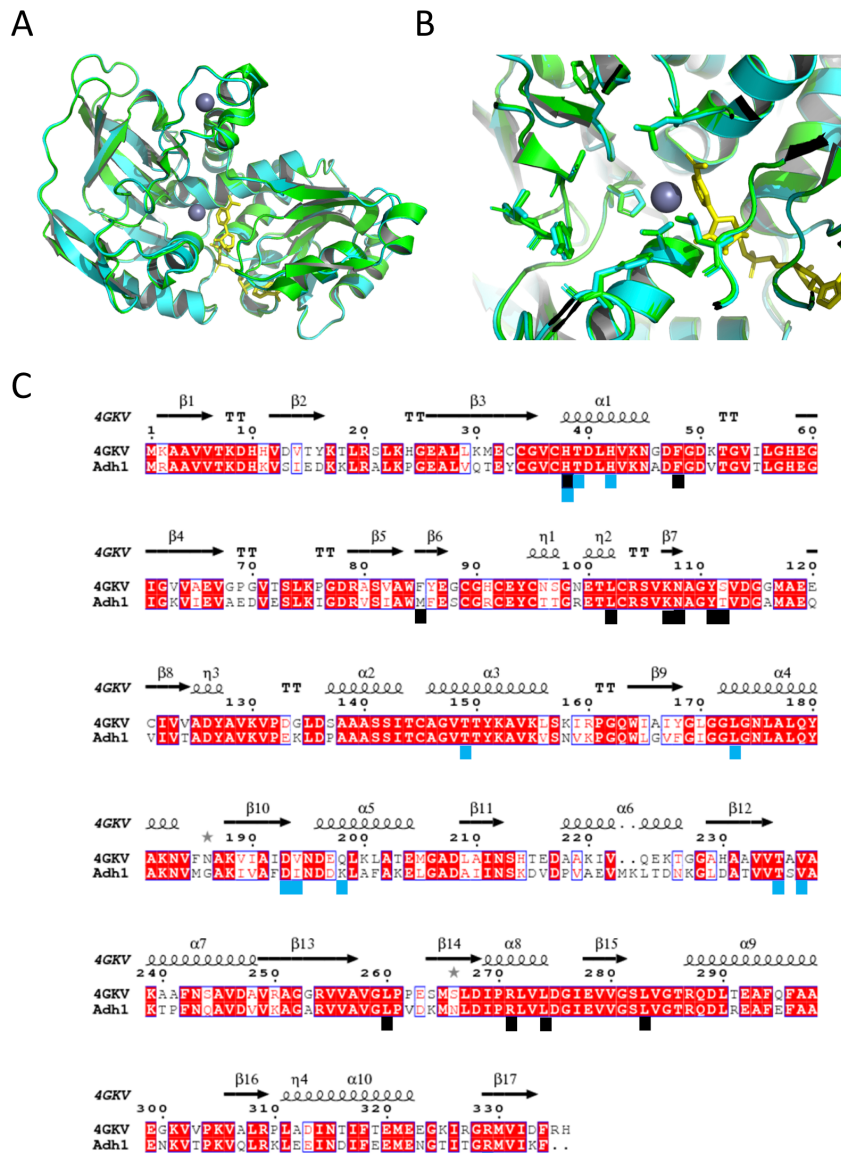


Figure S3. *E. coli* AdhP based homology model of *S. aureus* Adh1. Adh1 model predicted by Phyre2 using the *E. coli* ethanol-inducible MDR ethanol dehydrogenase/acetaldehyde reductase AdhP (PDB code: 4GKV) as template (1–4). 334 residues of Adh1 (99% sequence) were successfully modelled with high confidence (RMSD 0.606, over entire sequence). A) superimposition of Adh1 and AdhP showing high structure similarity: Adh1 colored cyan, AdhP colored green, NAD colored yellow and Zn colored violet. B) Active site of superimposed structures with residues critical for substrate binding shown as sticks. C) Sequence alignment of Adh1 and AdhP using the Clustal Omega web server and is displayed by ESPript 3 software (5). Invariant residues are highlighted in red. Overall sequence conservation is 68.7% identity and 88.6% similarity. Secondary structures of AdhP are shown. Boxes below the sequence indicate substrate (black) and coenzyme (blue) binding residues.

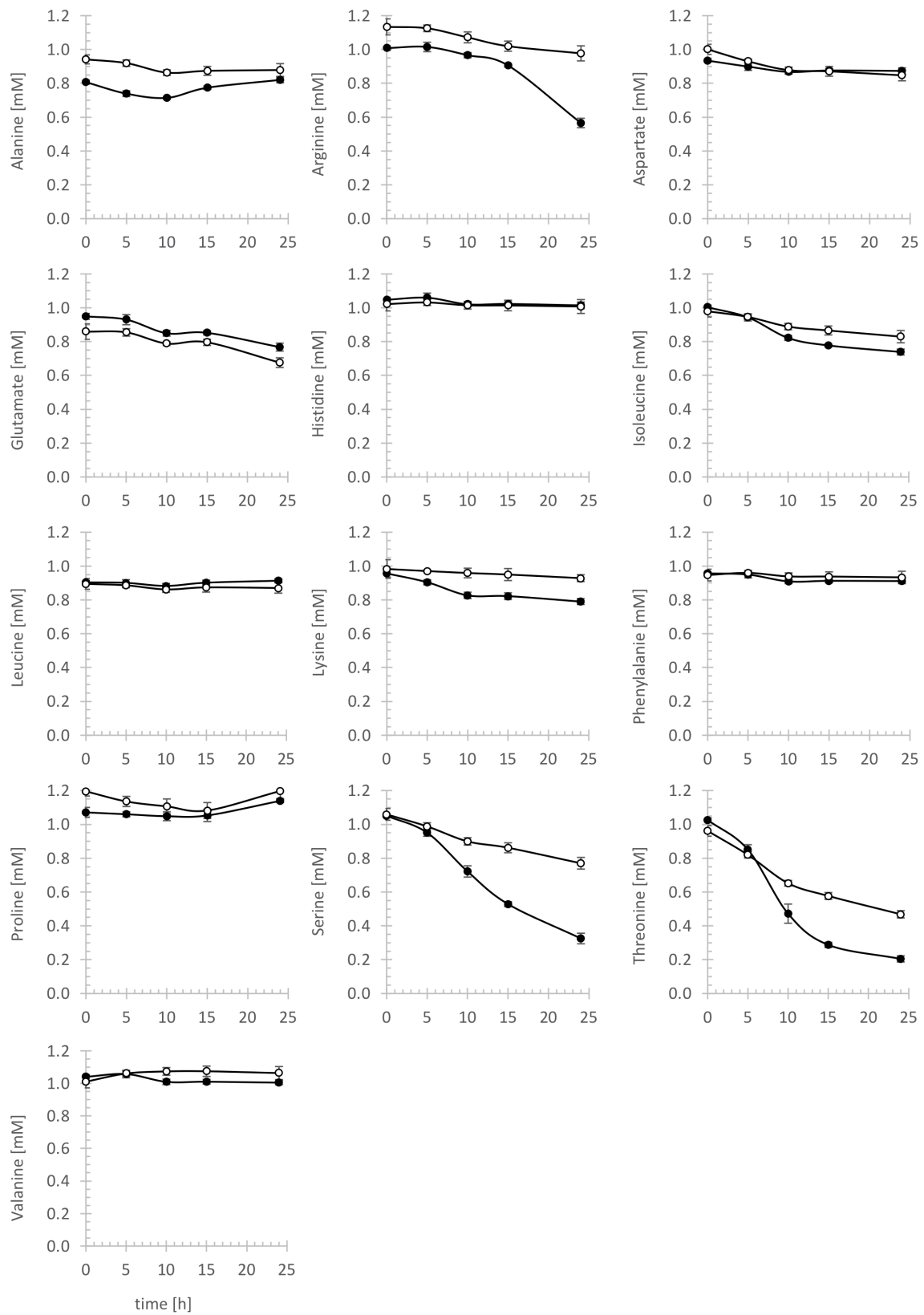


Figure S4. **Changes in extracellular amino acid concentrations.** (A) Concentrations profiles of amino acids supplements during anaerobic cultivation of *S. aureus* with either glucose (red line) or pyruvate

(green line) as major carbon and energy source. Results are mean values of five independent biological replicates. Corresponding standard deviation are shown as shade in transparent color. Values are means with standard deviation from four independent biological replicates. Statistics for amino acid profiles are summarized in Table S2.

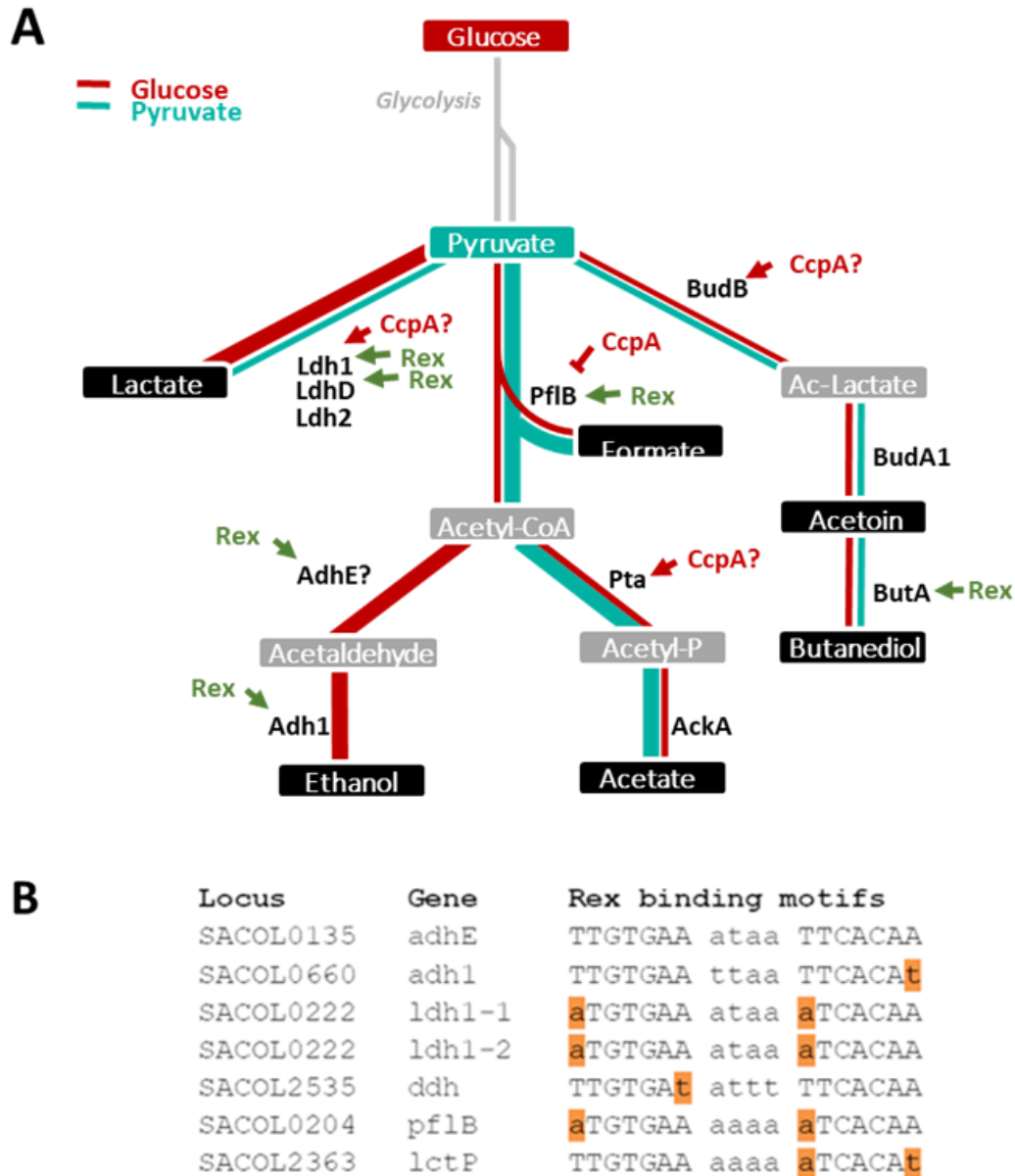


Figure S5. **Model of carbon source-dependent anaerobic gene regulation in *S. aureus*.** (A) A drop of the cellular redox potential leads to de-repression of Rex-regulated genes. If glucose is the major carbon source (red lines), lactate dehydrogenase 1 is by far the most abundant fermentation enzyme and the main secretion product is lactate, while only reduced amounts of acetate are produced. In the absence of a carbon source that can be anaerobically metabolized via glycolysis (turquoise line), glycolytic enzymes are not induced but Pfl is strongly upregulated in a Rex- and CcpA-dependent manner and acetate becomes the major secretion product. In addition, no ethanol is produced since this would divert valuable acetyl-CoA required for ATP production via Pta and AckA. Important regulatory proteins are indicated and motifs bound by Rex are shown in (B) with highlighted bases that

deviate from a perfect palindromic sequence. The question mark indicates potential indirect regulatory effects by CcpA.

Supplementary tables

Table S1. Summary of proteome data.

Table S2. Summary of exometabolome data.

Table S3 Oligonucleotides used in this study.

Table S3 Oligonucleotides used in this study.

Name	Sequence (5'-3')
ackA_for	GATGGGTATTCGTGCTTTCC
ackA_rev_T7	CTAATACGACTCACTATAGGGAGAATTCTCGCAGCATATGATCC
adh1_for	GTCTATCGCTTGGATGTTCCG
adh1_rev_T7	CTAATACGACTCACTATAGGGGAGACCGTCAAGCACTAATCTTGG
adhE_for	ATGCTCTAGCTGACAAAGGG
adhE_rev_T7	CTAATACGACTCACTATAGGGGAGATGTGCACTTGGATGGAATGC
budB_for	GTTAGGTGGCCAAGTGAAAC
budB_rev_T7	CTAATACGACTCACTATAGGGGAGACTTGATTGCGGAATAAGCCC
butA_for	CATTAGTAACTGGCGGAGCA
butA_rev_T7	CTAATACGACTCACTATAGGGGAGACAGGTTTACCTGCTTCTTCG
gapA2_for	GGGTAGAATTGGAAGAATGG
gapA2_rev_T7	CTAATACGACTCACTATAGGGGAGACCCCATTCAATATCATACCA
ldh1_for	CATGCCACACCATATTCTCC
ldh1_rev_T7	CTAATACGACTCACTATAGGGGAGAGCTGATACAGTCAATACGGC
ldh2_for	GGATCAAGCTATGCCTTTGC
ldh2_rev_T7	CTAATACGACTCACTATAGGGGAGAGCTTGTGACCAAACCTGCAAG
ldhD_for	CGCGTGATTATGAGAAAGAG
ldhD_rev_T7	CTAATACGACTCACTATAGGGGAGAGCGTTTAAACCACCTTCAAC
pdhA_for	GGTTTCTATGCACCAACTGC
pdhA_rev_T7	CTAATACGACTCACTATAGGGGAGAGCGGTACCGTGCTTCTTTAG
pflB_for	GGTGCAGCAATGAGTTTAGG
pflB_rev_T7	CTAATACGACTCACTATAGGGGAGATTTGGACCAAACCTGTGCACC
pta_for	CGACGTAAAGGTAAAGCGAC
pta_rev_T7	CTAATACGACTCACTATAGGGGAGAGCAACACCTGGTACAATCGC

References

1. Thomas LM, Harper AR, Miner WA, Ajufo HO, Branscum KM, Kao L, Sims PA. 2013. Structure of *Escherichia coli* AdhP (ethanol-inducible dehydrogenase) with bound NAD. *Acta Crystallogr Sect F Struct Biol Cryst Commun* 69:730–732. doi:10.1107/S1744309113015170.
2. Karlsson A, El-Ahmad M, Johansson K, Shafqat J, Jörnvall H, Eklund H, Ramaswamy S. 2003. Tetrameric NAD-dependent alcohol dehydrogenase. *Chem Biol Interact* 143-144:239–245. doi:10.1016/s0009-2797(02)00222-3.
3. Kelley LA, Mezulis S, Yates CM, Wass MN, Sternberg MJE. 2015. The Phyre2 web portal for protein modeling, prediction and analysis. *Nat Protoc* 10:845–858. doi:10.1038/nprot.2015.053.
4. Shafqat J, Höög JO, Hjelmqvist L, Oppermann UC, Ibáñez C, Jörnvall H. 1999. An ethanol-inducible MDR ethanol dehydrogenase/acetaldehyde reductase in *Escherichia coli*: structural and enzymatic relationships to the eukaryotic protein forms. *Eur J Biochem* 263:305–311. doi:10.1046/j.1432-1327.1999.00323.x.
5. Robert X, Gouet P. 2014. Deciphering key features in protein structures with the new ENDscript server. *Nucleic Acids Res* 42:W320-4. doi:10.1093/nar/gku316.